ORIGINAL SCIENTIFIC PAPER

CROATICA CHEMICA ACTA

Croat. Chem. Acta **2022**, *95*(3), 101–110
Published online: April 11, 2023
DOI: 10.5562/cca3939

HKD 1926

Copper(II) Coordination Compound with 2-Oxonicotinate: Synthesis, Spectroscopic and Electrochemical Studies

Ivana Škugor Rončević,* Nives Vladislavić, Marijo Buzuk

Department of General and Inorganic Chemistry, Faculty of Chemistry and Technology, University of Split, Ruđera Boškovića 35, 21000 Split, Croatia
* Corresponding author's e-mail address: ivana.skugor-roncevic@ktf-split.hr

RECEIVED: November 15, 2022 ✶ REVISED: February 3, 2023 ✶ ACCEPTED: February 5, 2023

Abstract: Metal organic frameworks (MOFs) are gaining interest for technological purposes due to their intriguing open structure properties such as ion exchange, catalytic properties and application as sensors. To prepare coordination compounds with desired properties, the choice of organic ligand is crucial. This work demonstrates the hydrothermal synthesis of a copper(II) coordination compound with 2-hydroxynicotinic acid. Characterization was based on elemental analyses, ESI-MS, MALDI-TOFMS, FT-IR spectra, thermogravimetric analysis (TGA), and cyclic voltammetry. Electrochemical characterization of the compound prepared was also carried out to find a sensitive and simple method to improve the determination of biologically active thiol substances. From the rectangular voltammetry results, a linear response between 0.2 and 20 μM was obtained with an estimated detection limit of 0.09 μM.

Keywords: coordination compound, copper(II), 2-hydroxynicotinic acid, Fourier transform infrared spectroscopy, cyclic voltammetry, cysteine, square wave voltammetry.

INTRODUCTION

THE last decade has resulted in increased interest in metal-organic polymer structures, based on metal-ligand and non-covalent interactions. Interesting and diverse structures obtained by different approaches in synthesis have found a place and potential application as functional materials, with a clear purpose.[1,2] The final organic-inorganic hybrid crystalline porous materials are depending predominantly on organic anions, metals cations, pH values, reaction temperatures, solvent, and important, but not the last factor is certainly radiation (light).[3–5] The first and most important step in structuring coordination polymers is the selection of an appropriate ligand, organic linker, with a defined coordination number, most commonly neutral N-donor or anionic O-donor ligands. In combination with the cation of *d*-block metals, which possess chemically active *d*-orbital electrons, they give a large number of MOFs with an extremely interesting atomic-level structural uniformity, adjustable porosity, and chemical functionality.[6–8] Neutral organic linkers are crucial for adapting the topology of coordination frameworks, as well as the possibility of changing the configuration of the coordination polymer.[9–11]

A suitable organic ligand, such as 2-hydroxynicotinic, has many advantages in coordination acids: multiproton acceptor-donor sites make it the preferred multidentate ligand. It is solid and offers the possibility of multiple hydrogen bonds. 2-Hydroxynicotinic acid displays various bonding geometries duo to eight coordination modes, resulting in the presence of the carboxylate and the phenolic hydroxyl group. Also very important fact, specified groups in 2-Hydroxynicotinate can serve as a ma mediator magnetic exchange when light and is linked to metal magnetic centers.[12,13]

In this work, Cu was selected as a metal with different coordination geometries and affinities to different organic ligands.[14–16] In humans, copper is present in the liver, muscles and bones. Copper is also used as a fungicide in agriculture, has anti-biofouling, antimicrobial, antifungal and antiviral properties and applications, has biostatic properties, that is, bacteria do not grow on it. An

interesting fact is that copper bracelets can be used to cure arthritis symptoms.[17] Copper complexes play an important role in catalyzing enzymatic activity, and some copper(II) carboxylates are used as pharmaceuticals.[18] In addition to the well-known fact that endogenous copper plays an important role in many biochemical processes in the metabolism of all living cells, pyridinecarboxylic acids as well as their derivatives also play an important role.[19,20] Pyridinecarboxylic acids and their derivatives form a significant group of anthelmintics and vitamins.[19] Nicotinic acid, pyridine-3-carboxylic acid (also known as vitamin B_3 or niacin) is converted to nicotinamide adenine nucleotide (NAD), which in the two-electron transfer in organisms serves as an intermediate.[21–23] Vitamin B_3 is used in clinical use to prevent atherosclerosis, and for the treatment of pellagra resulting from its insufficient intake.[22,23] Some chronic diseases such as anemia, headache, fatigue, nausea, and skin infections are due to vitamin B_3 deficiency, but excessive intake causes toxic effects such as maculopathy leading to blindness or diabetes mellitus.[17]

Copper-nicotinic acid complex has been successfully used to treat fatty liver (fat deposits in liver cells and causes problems in the structure and functions of the liver) in rats.[24] Cu(II) complexes with nicotinic acid also showed antimicrobial activity against Bacillus subtilis and super oxide dismutase (SOD) mimetic activity.[25] Cyclic voltammetry (CV) is one of the most efficient and versatile electrochemical techniques that can be used to study the mechanisms and kinetics of redox systems of numerous electroactive species, including complexes. The main parameters of CV are the magnitude of the peak currents, i_{pa} and i_{pc}, and the potentials at which the peaks occur, E_{pc} and E_{pa}. In an ideal system, $|E_{pc} - E_{pa}|$ for reversible peak currents (at a ratio $i_{pa} / i_{pc} = 1$) is 59 mV for a 1-electron process and 30 mV for a 2-electron process.[26] Various modified electrodes have been prepared from carbon materials, metal nanoparticles, metal-organic frameworks, etc. (Table 1). It is reported, that when carbon nanotubes (CNT), were first observed by Iijima in 1991., are used as electrode or electrode modifiers their ability to act as a mediator in electron transfer reactions is increased, thanks to the exceptional characteristics of CNT as new material.[35,36] Carbon nanomaterials have given many advantages to the final design of the modified electrode surface, the most important of which is the improvement of electron transfer reactions, "faster electron transfers kinetics" that is commonly interpreted in terms of "electrocatalysis" of carbon nanomaterial.[37]

Cysteine is a nonessential amino acid that contains sulfur in the reactive thiol group (-SH). It can form disulfide bridges with another cysteine within the protein chain or between protein chains. It is incorporated into proteins and is a precursor in the synthesis of essential amino acids. In this sense, the biological role of cysteine is extremely important. Qualitative and quantitative analysis is very difficult because thiol is subject to oxidation. This is where electrochemical methods come into focus as simple, fast and very sensitive methods, and their application is possible precisely thanks to their antioxidant properties.[32] Table 1 shows the various electrochemical methods used to determine Cys-SH. The catalytic activity (electron transfer) is significantly influenced by the design of the electrochemical sensor, *i.e.*, by the appropriate modification of the carbon material. With a suspension of SWCNT and Cu(II) complex **1** modified glassy carbon electrode (GC|SWCNT|**1** electrode), a lower detection limit, shorter deposition time and wider linear range were obtained. This significantly shortens both the duration of analysis and the price, and makes the method environmentally friendly compared to other methods.

Table 1. A brief literature review - the comparison of the analytical performance of the GC|SWCNT|**1** electrode with different carbon-based materials and modified electrodes in the literature.

Electrode	Method	*E*p (V) vs Ag/AgCl	LOD / μM	Linear range / μM	Sensitivity / nA μM^{-1}	Ref.
Bulk carbon electrodes modified with cobalt phthalocyanine	CV, CA	0.40	0.2	1–12	8.89	[27]
Nile blue modified GC	CA	–0.45	1.3	10–250	NA	[28]
MWCNT modified GCE	Amperometry	0.18	5.4	10–500	3	[29]
Pt nanoparticles/poly(o-aminophenol) film on GCE	Amperometry	0.41	0.08	0.4–6300	NA	[30]
Catechol on GC	CV	0.22	6.0	15–50	NA	[31]
Bi film on different crbon based electrodes	SWCSV	–0.40	0.028	1–10	398	[32]
Copper-organic frameworks modified with gold nanoparticles on GCE	SWV	0.15	0.0004	0.0015–10.5	780	[33]
Hydroxyapatite on glassy carbon electrode	SWCSV	0.10	0.033	1–10	327	[34]
GC modified with SWCNT|**1** suspension	SWV	0.15	0.09	0.2–20	1722	Our work

CA: Chronoamperometry; CV: Cyclic voltammetry; DPV: Differential pulse voltammetry; SWCSV: square wave cathodic stripping voltammetry; SWV: square wave voltammetry

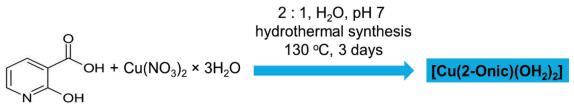

Scheme 1. Preparation of [Cu(2-Onic)$(OH_2)_2$] (**1**) under hydrothermal conditions.

Synthesis, spectral properties and electrochemical characterization as well as crystal structures of 1D cationic Co(II) or Ni(II) coordination compounds with 4,4'-bipyridine, with empirical formulae {[Co$(OH_2)_4$(4,4'-bpy)](6-OHnic)$_2$ × 2 H_2O}$_n$ and {[Ni$(OH_2)_4$(4,4'-bpy)](6-OHnic)$_2$ × 2 H_2O}$_n$ were described in our previous publications.[38] A review of the literature revealed a number of papers on the topic of copper pyridine carboxylate coordination polymers prepared by solvothermal conditions. The advantages of pyridine carboxylate ligands are the tendency to bind metal centers with pyridyl and carboxylate groups, which result in 1D types of structures and ultimately the creation of large porous 3D networks.[20]

To further understand the coordination chemistry of a solid N-donor ligand that additionally contains a carboxyl group, we synthesized and characterized copper(II) coordination compound with 2-hydroxynicotinic acid (2-OHnicH), namely [Cu(2-Onic)$(OH_2)_2$], **1** (Scheme 1). The compound was characterized by elemental analysis, electrospray ionization mass spectrometry (ESI-MS), matrix-assisted laser desorption/ionization time-of-flight mass spectrometry (MALDI-TOFMS), infrared spectroscopy (IR), and thermogravimetric analysis (TGA). In addition, the electrochemical properties of the compound were also carefully investigated. Coordination compound **1** modified electrode was also used for the determination of cysteine (Cys- SH) as a sensor material.

EXPERIMENTAL

Physical Measurements

The used instruments are:

- Elemental analyses (C, H and N): Carlo Erba Microanalyzer at the Microanalytical Laboratory of the University of Vienna, Austria.
- Mass spectra: UHPLC-DAD-MS/MS (Ultimate 3000RS equipped with DAD and TSQ Quantis MS/MS detectors, along with H-ESI ion source Thermo Fischer Scientific, Waltham, MA, USA) using Hypersil GOLD C18 column (3.0 µm, 3.0 × 100 mm, Thermo Fischer Scientific, Waltham, MA, USA). Following conditions: Source fragmentation: 0 V; Positive polarity: 3500 V; Sheath Gas: 60; Aux Gas: 15; Sweep Gas: 2; Temperature of the evaporator: 350 °C; temperature of the ion transfer tube: 350 °C. Scanning was performed in Full Q1 scan mode: 50–1000 *m* / *z*; Scan rate: 1000 Da/sec; Q1 resolution: 0.4 FWHM.
- Electrospray ionization mass spectrometry (ESI MS) - MALDI-TOF mass spectra: TimsTOF flex (Laserpower 1%, Positive polarity) at Mass Spectrometry Centre of the Faculty of Chemistry of the University of Vienna. Scanning was performed in 300–2200 *m*/*z*.
- Fourier transform infrared spectroscopy (FTIR): by the KBr method on a Shimadzu IRAffinity-1 FTIR spectrometer in the range 4000–400 cm^{-1}.
- Thermogravimetric measurement analyses (TGA): Shimadzu DTG-60H analyzer heated from room temperature to 800°C in a stream of synthetic air at a heating rate of 10 °C min^{-1}. A Pt semi-macro crucible (6 mm Ø × 5 mm) was used and the mass of the sample was 7.186 mg.
- Electrochemical measurements - Cyclic voltammetry (CV) and Square wave voltammetry (SWV): Autolab PGSTAT 302N potentiostat controlled by GPES 4.9 electrochemical software from Eco-Chemie

Synthesis of Coordination Compound, [Cu(2-Onic)$(OH_2)_2$]- Cu(II)-Complex

A mixture of distilled water (6 mL), $Cu(NO_3)_2$ × 3 H_2O (0.043 g, 0.1797 mmol) and 2-hydroxypyridine-3-carboxylic acid (0.050 g, 0.3594 mmol), the pH of which was adjusted to 7 with 8 % NaOH solution, was transferred to a Teflon-lined autoclave and heated to 130 °C for 3 days. After 72 hours' autoclave was left at room temperature for slow cooling. The blue crystals of **1** were obtained with a yield of 56 %. Anal. Calcd. for $C_6H_8NO_5Cu$ M = 236.68 g mol^{-1} (%): C, 30.45; H, 2.98; N, 5.92; O, 33.80. Found: C, 30.76; H, 2.16; N, 6.24; O, 29.23 %. FTIR (Standard KBr technique, cm^{-1}; w, weak; m, medium; s, strong): 3481 (m), 3422 (m) [ν(O–H)], 1614 (s) [$\overline{\nu}(COO^-)]_{as}$, 1566 (s), 1476 (s), 1390 (s) [$\overline{\nu}(COO^-)_s$], 1353 (m), 1255 (m), 1230 (m), 1210 (m), 1161 (w), 1060 (w), 925 (m), 782 (s), 671 (m), 613 (m), 585 (w), 542 (w).

ESI–MS (*m*/*z*) (%): 282 (100) [CuL$(H_2O)_2$], 381 (100) 2 $Na^+[Cu(L)_2]^{2-}$, 723 (100) **{**[Cu$(L)_2(H_2O)$]**}$_2$;** MALDI-TOF-MS (*m*/*z*): 563 [CuL$(H_2O)_2]_2$.

Preparations Electrodes Suspensions, Namely SWCNT and SWCNT|1

Pure **SWCNT** (5 mg of SWCNTs, diameter 0.7–0.9 nm, with ≥ 93 % carbon as SW), or modified **SWCNT|1** (5 mg of each, SWCNT and Cu(II)-complex **1)** was dispersed for 10 h, in 10 mL of *N, N*-dimethylformamide, using an ultrasonic bath (Bandelin SONOREX, model RK 31), to obtain 0.5 mg mL^{-1} SWCNT (SWCNT|**1**) suspension.

Electrochemical Measurements

All electrochemical measurements were performed in a 0.1 mol L^{-1} KNO_3.

A three-electrode system (Ag/AgCl reference electrode, Pt wire counter electrode, and glassy carbon (GC) working electrode (K-type, diameter 6 mm) modified with a prepared suspension was used for the electrochemical measurement. The GC surface was mechanically polished to 50 nm before modification with a fine-grained alumina suspension, sonicated in distilled water, and rinsed with ethanol and distilled water. GC modified with SWCNT (SWCNT|**1**) suspension was prepared by drop-casting of 15 µL of the prepared suspension on a GC surface and left to evaporate at 50 °C.

At the SWCNT and SWCNT|**1** electrodes, the electrochemical behavior of coordination compound **1** was studied by recording CVs at room temperature over a wide potential range (−1.0–1.2 V, vs. Ag/AgCl) and with a voltage sweep of 10 mV s^{-1}, respectively. Measurements were made starting from E_{ocp} in the anodic direction to +1.2 V, then in the reverse cathodic direction to −1.0 V and back to E_{ocp}.

RESULTS AND DISCUSSION

To study the active species of synthesized complexes high-resolution ESI MS mass spectra were recorded. The ESI mass spectra of the coordination compound **1** recorded in positive ion mode showed three main mass-to-charge ratio peaks (Figure 1.).

The most abundant peak, at *m/z* 282 amu is assigned to $[Cu(L)(H_2O)_2]$, while the second at *m/z* 381 amu to

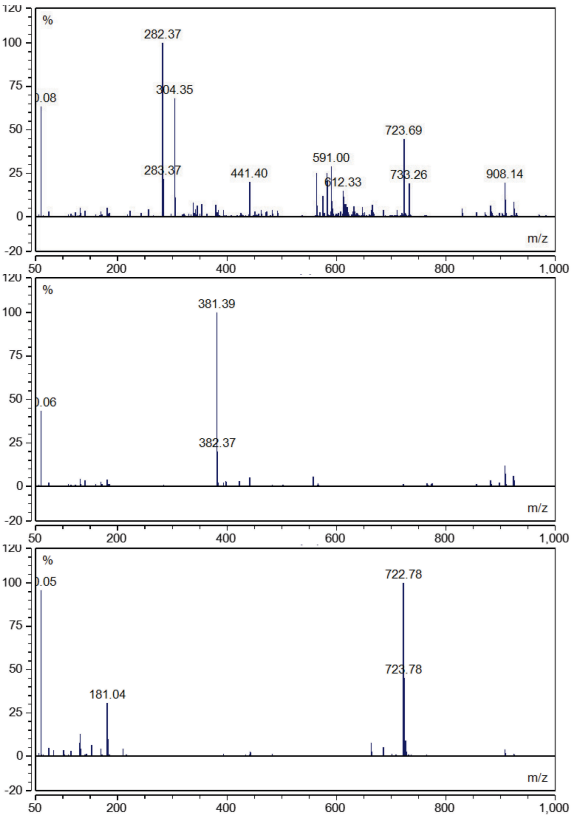

Figure 1. Full ESI mass spectrum of the coordination compound **1**.

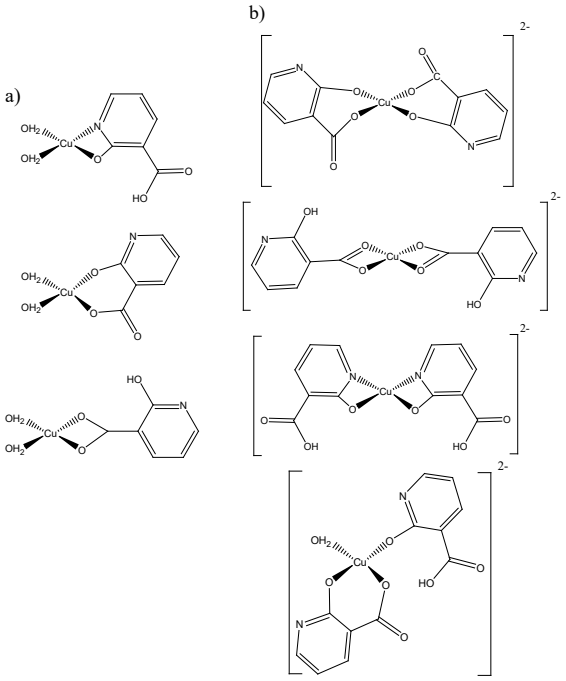

Scheme 2. Possible structure for m/z 282 (a) and for *m / z* 381 (b)

2 $Na^+[Cu(L)_2]^{2-}$ ions. The metal oxidation state and coordination number are chemically reasonable, however, there are more possible structures for an *m/z* value 282 *i.e.* 381 as shown in Scheme 2.

The intensities of these peaks give the idea of the stabilities of the complex compound. The third most abundant peak, at *m/z* 723 amu is assigned to $\{[Cu(L)_2(OH_2)]\}_2$ and it is assumed to have a "paddle wheel" structure (Scheme 3.).[39]

It should also be noted that the second peak (at *m/z* 381 amu) assigned to 2 $Na^+[Cu(L)_2]^{2-}$ ions could be a consequence of dissociation of water molecule ligands under the conditions of ESI-MS, as observed in other copper(II) complexes.[40]

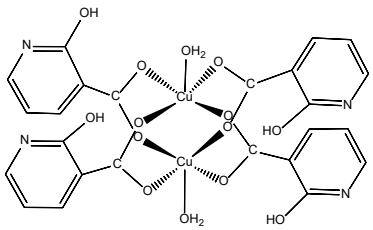

Scheme 3. Possible "paddle wheel" structure for *m / z* 723.

To more accurately determine the active chemical specie of the complexes, *ie.* the coordination geometry around copper(II) in **1**, characterization by MALDI-TOFMS analysis was utilized. Figure S1 in the Supplementary Materials shows ESI spectra for the target complex with low intensity. The high-resolution ESI MS(+) mass spectra of the complex compound **1** showed the one main most abundant peak (at *m*/*z* 563 amu) attributed to $[Cu(L)(H_2O)_2]_2$, several other highly charged multi-isotopic species observed and additional low charge state species, possibly from impurity. The exact mass and isotopic distribution are in good agreement with the calculated spectra. MS spectra can be interpreted as the spectra of the expected ions of the products with the proposed structure - no significant background noise.[41]

The FT-IR spectra of coordination compound **1** (Figure S2 in the supplementary materials) show broad bands of high intensity in the range from 3300 cm^{-1} to 3650 cm^{-1}, corresponding to the stretching vibration of OH and proving the presence of water molecules, which is in agreement with the results of elemental analyses.[18] The bands at 1390 cm^{-1} and 1614 cm^{-1} were assigned to the symmetric and asymmetric vibrations of OHnic carboxylates, respectively. The information on the carboxyl-binding mode of the complexes provides the difference between the antisymmetric stretching and symmetric stretching (*Δ*) compared to *Δ* of compounds with ionic carboxyl groups. The larger difference between the antisymmetric stretching and the symmetric stretching of the carboxylate ($\Delta = \nu_{as}(COO^-) - \nu_s(COO^-) = 224$ cm^{-1}) indicates a monodentate, chelating asymmetric coordination of the carboxyl group. The *Δ*-value in this case is comparable to that of unidentate complexes.[42] On the other hand, the splitting of the $\nu_{as}(COO^-)$ assigned band in the FT-IR spectra of complex compound **1** is more typical for the *O*, *O*-asymmetric chelating coordination of the carboxyl groups of 2-OHnicH.[22] The band at 1476 cm^{-1} corresponds to the ν(C=N) stretching of the pyridine ring of the ligand.[18] The positions of the band corresponding to the skeletal vibrations of the pyridine ring at 781 cm^{-1} and 1053 cm^{-1} for the free ligand (Figure S3 in the Supplementary Materials) are almost the same wavenumber; 782 cm^{-1} and 1060 cm^{-1}, for coordination compound **1,** respectively. This suggests that the coordination of the ligand to the central metal ion was not achieved via the nitrogen atom of the pyridine ring. From the position of the band which corresponds to ν(C–O) stretching vibration of Ph–OH group in free acids which is shifted for coordination compound **1** by about 23 cm^{-1} to higher wavenumbers (1187 → 1210 cm^{-1}) can assume the deprotonated Ph–O^- group and monodentate coordination through a phenolate oxygen atom.[43] The bands in the range 1350 – 1200 cm^{-1} at wavenumbers 1255, 1230, and 1161 cm^{-1} were attributed to the $\bar{\nu}$(C–O) of the 2-OHnicH ligand.

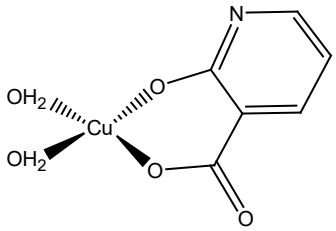

Scheme 4. A possible structure for the coordination compound **1**.

Furthermore, the FT-IR spectra show characteristic bands at approximately 671 and 613 cm^{-1} which could be attributed to the "rocking and wagging" of coordinated water molecules, which go in favor, as well as all above stated, of a possible structure for the coordination compound **1** as shown in Scheme 4.

The thermal behavior of coordination compound **1** was studied by TGA (Figure S4 in the supplementary materials). The complex compound undergoes complete endothermic and exothermic decompositions in three step. The first step in the range of 31–190 °C corresponds to the endothermic elimination (DTA maximum: 139 °C) of the free water molecule (observed: 6.1 %; calculated: 6.3 %). Shortly thereafter, between 190 and 450 °C, there is a mass loss of 67.2 % (DTA maximum: 330 °C, calculated: 67.4 %) in the second, not well resolved phase of the thermal analysis, which is due to the endothermic removal of water molecules from the pores and as ligands (peak at 286 °C) and of the one 2-hydroxynicotinic acid ligand (2-OHnicH) in an exothermic process (peak at 330 °C). The loss of water at higher temperatures may indicate that the water molecules participate in strong and extensive hydrogen bonding.[44] Finally, the degradation of the structure led to the formation of CuO (observed: 30.4 %; calculated: 28.0 %) at 800 °C. The last decomposition step is exothermic (peak at 347 °C), which is consistent with the formation of the thermodynamically stable copper(II) oxide during the complete decomposition of coordination compound **1**.

Electrochemical Characterization

ELECTROCHEMICAL CHARACTERIZATION OF THE $[Cu(2\text{-Onic})(OH_2)_2]$ (1)

A series of cyclic voltammograms (Figure 2) for electrochemical characterization of the prepared complexes was performed on the bare electrode (GC), the modified electrode (GC|SWCNT|**1**), and the GC electrode with addition of the complex in solution (GC|SWCNT|2-OHnicH). Three CV cycles were recorded in the potential range of –1.0 V–+1.2 V (ν = 10 mV s^{-1}). Measurements were made starting from E_{ocp} in the anodic direction to +1.2 V, then in the reverse cathodic direction to -1.0 V and back to E_{ocp}. Figure 2

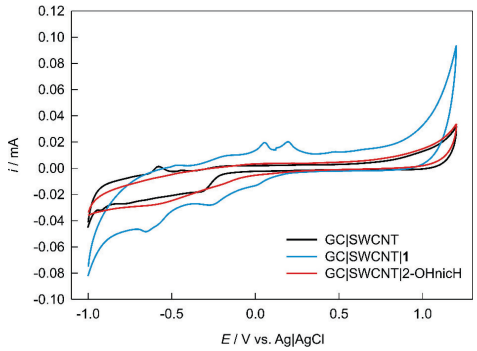

Figure 2. CVs recorded on modified GC electrodes: GC|SWCNT| (without complex), (GC|SWCNT|**1**) (with prepared complex) and GC|SWCNT|2-OHnicH (without complex and with the addition of 2-OHnicH into electrolyte). v = 10 mV s^{-1}.

shows cyclic voltammograms (second CV cycle) recorded on a GC modified with a suspension of SWCNT alone, GC|SWCNT|, a GC|SWCNT|**1**, and GC|SWCNT|2-OHnicH.

As can be seen in Figure 2, in the studied polarization range, the broader CV response was observed in the case of the GC|SWCNT|**1** electrode with respect to the CV response of the GC|SWCNT| electrode. In addition, it is important to emphasize that the current increases tenfold for the GC|SWCNT|**1** electrode compared to the GC|SWCNT| electrode. This indicates differences in the rate of electron transfer, *i.e.*, the presence of |SWCNT|**1** at the electrode surface enhances electron transfer.[37] Cyclic voltammograms recorded at the GC|SWCNT|**1** electrode during the anodic scan show two quasi-reversible oxidation current peaks at potentials of 0.06 V and 0.20 V, which are attributable to the oxidation of the central metal ion Cu into Cu^+ and Cu^+ into Cu^{2+}, while successive reduction of the metal center $Cu^{2+} \rightarrow Cu^+ \rightarrow Cu$ is observed in the cathodic scan at potential of 0.01 V. The peak at a potential of 0.47 V can be attributed to the oxidation of the ligand 2-OHnicH, while the reduction of the ligand occurs in the reverse part of the cyclic voltammogram at a potential of –0.65 V (see Scheme 5). A large DE_p value for the ligand redox reaction, DE_p = $E_{p,a}$ – $E_{p,k}$ = 1.11 V, indicates an irreversible process at a given scan rate.[45]

In addition, the oxidation current peak at a potential of –0.48 V and the reduction current peak at a potential of

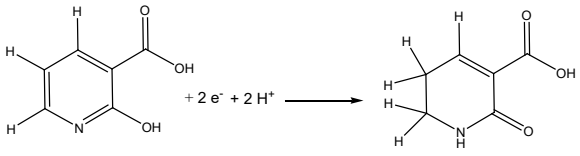

Scheme 5. Preparation of [Cu(2-Onic)$(OH_2)_2$] (**1**) under hydrothermal conditions.

–0.26 V refer to the oxidation or reduction of the electrode material or the SWCNT modifier of the GC electrode.

THE ELECTROCHEMICAL BEHAVIOR OF Cys-SH ON GC|SWCNT|1 ELECTRODE

With the aim of using GC|SWCNT|**1** electrode as the sensor for electrooxidation and the detection of Cys-SH, the electrochemical properties of the GC|SWCNT|**1** electrode was studied by cyclic voltammetry containing Cys-SH. Figure 3 shows the cyclic voltammograms recorded between -0.05 V and 0.8 V for the GC|SWCNT|**1** electrode in the absence of Cys-SH and in the presence of Cys-SH; 1 × 10^{-4}, 5 × 10^{-4} at a potential scan rate of 25 mV s^{-1}. Increase anodic current values of the GC|SWCNT|**1** electrode for the successive addition of Cys-SH, compared to the CV response in the absence of Cys-SH, is due to the high electrostatic interaction between Cys-SH and Cu(II) from the SWCNT|**1** modified GC electrode and the presented reaction for the Cys-SH oxidation (Scheme 4.). This result indicates that GC|SWCNT|**1** electrode has the ability to increase the rate of the electron transfer process for the oxidation of Cys-SH. Thus, a pronounced anodic peak occurred at the GC|SWCNT|**1** electrode at a potential of 0.4 V, corresponding to the irreversible oxidation reaction of Cys-SH, and a current of 0.4 mA was obtained for the addition of 1 mM Cys-SH to the solution of an electrolyte (green curve). It was found that the position of the oxidation peak did not change, indicating a reaction on the surface of the modified electrode catalyzed by the presence of copper as an intermediate in electron transfer. It can be concluded that the copper from the complex can serve as an adsorption-desorption site without changing the position in the complex.[40]

Considering obtained results and literature data according to which the thiol (SH) group of Cys-SH shows a

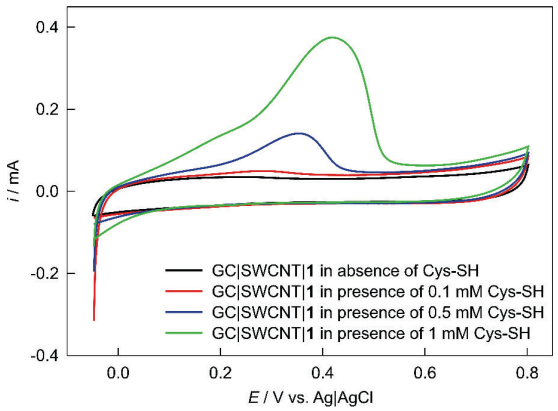

Figure 3. CVs recorded at the GC|SWCNT|**1** electrode in the absence of Cys-SH and in the presence of Cys-SH; 0.1, 0.5, and 1 mM. v = 25 mV s^{-1}.

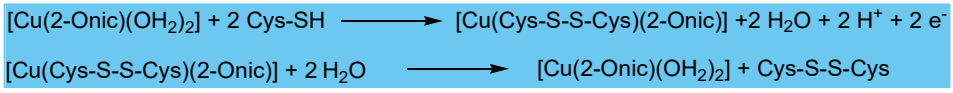

Scheme 6. The possible semi-reduction reaction of the ligand, 2-OHnicH at GC|SWCNT|**1** electrode.

strong tendency to oxidation and easily forms a disulfide bond, (S–S–) dimer, the electrochemical oxidation of Cys-SH on GC|SWCNT|**1** can be written as shown in Scheme 6.

After adsorption of Cys-SH on the surface of the GC|SWCNT|**1** electrode, Cu(II) ions from complex compound **1** complex with Cys-SH as a result of the aqua-ligand substitution reaction with Cys-SH to form a dimeric $Cu(S\text{-}Cys)_2$ complex, which is oxidized to cystine in the next step and Cu(II) returns to complex compound **1** (Scheme 6).

ANALYTICAL APPLICABILITY OF THE GC|SWCNT|1 ELECTRODE

The analytical applicability and sensitivity of the GC|SWCNT|**1** electrode for the detection of Cys-SH were investigated. Using literature data and observing the influence of step potential (ΔE_s), frequency (f), and pulse amplitude (ΔE_p) on peak oxidation currents (I_p), an optimal SWV procedure was determined (Figure S5 A and B in the supplemental materials). For all ΔE_s values studied, a frequency increase up to 35 Hz leads to an increase in I_p. At frequencies above 35 Hz, the current peaks decrease, which is due to a kinetic constraint. As shown in Figure S5B, I_p is practically linear with E_p at values below 50 mV. SWV analysis, performed by the standard addition method, was performed at an initial deposition potential of 150 mV and a deposition time of 120 s in stirred solution, followed by 30 s in unstirred solution. After piletion, SWV was performed in unstirred solutions from 0.15 V to 0.6 V at 35 Hz, a pulse amplitude of 45 mV, and a step potential of 15 mV. On these terms, we were able to ensure good electrode response and great sensitivity and reproducibility of measurements. All measurements were performed at room temperature in 0.1 M KNO_3 solution. The pH was set at 4.0 (with 0.1 M HNO_3 solution) because Cys-SH allows high peak anodic currents at this pH since it is protonated.[33] For the SWV detection of cysteine, an accumulation potential of 0.15 V was chosen to ensure the formation of the $Cu(S\text{-}Cys)_2$ complex while avoiding the reduction of Cu(II). Figure 4 shows square waive voltammograms (SWVs) obtained at increasing Cys-SH concentrations, and the curves shown are background subtracted oxidation currents. Calibration plots of the GC|SWCNT|**1** electrode versus Cys-SH were extracted from the SW voltammograms, and the results are shown in the Appendix of Figure 4.

Figure 4 shows the dependence of the current I_{pa} on the increase in the concentration of the analyte added to the solution, from 0.2 to 60.0 μM. A linear calibration curve is obtained for 0.2-20 μM Cys-SH with a slope of 1.722 μA μM^{-1}. The mathematical relation among the analytical signal and concentration was $I_p(A) = 0.9560 + 1.722\ c_{Cys\text{-}SH}(M)$, and the correlation coefficient was 0.978. Using the criteria of $3 \times s_b/m$ and $10 \times s_b/m$, where s_b is the standard deviation of the axis intercept and m is the sensitivity, a limit of detection (LOD) and a limit of quantitation (LOQ) were calculated, which are 0.090 μM and 0.277 μM, respectively. Slightly inferior sensitivity for the detection of cysteine was found for the higher range of concentration (20–60 μM).

The slight change in sensitivity observed at higher cysteine concentrations and relatively good linearity could be due to adsorbed cysteine on the electrode surface and related to possible passivation of part of the surface or changes in complex morphology due to the interaction of copper and thiol compounds.[34]

For the successful application of copper coordination complexes, it is necessary to implement interferences study of some species, especially those present in biological samples. Due to the properties of copper to interact easily with thiol contain compounds, possible interferences are precisely from these types of analytes. By adding the appropriate amount of lauric acid, EDTA, vitamin C, L-alanine, isoleucine and glutathione to a solution containing 10.0 μM cysteine, with an interference criterion of ±5 % peak current error, we obtained sufficient information on possible

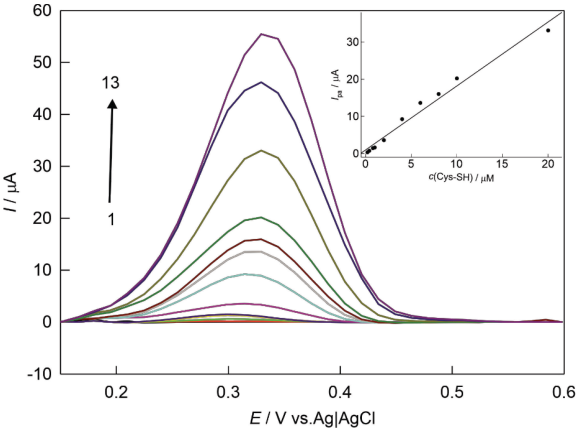

Figure 4. a) SW voltammograms of diverse Cys-SH concentrations (0.2-60.0 mM) at GC|SWCNT|**1** electrode (E_{dep} = 150 mV; t_{dep} = 120 s; f =35 Hz; ΔE_p = 45 mV; ΔE_s = 15 mV. b) Inset: Calibration plot.

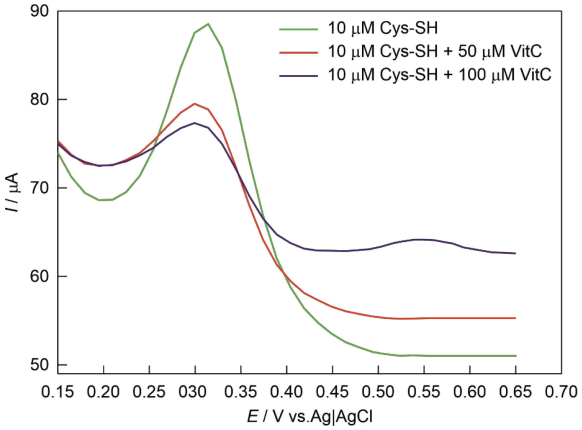

Figure 5. SW voltammograms of 10.0 μM Cys-SH in the presence of vitamin C (50.0 μM, 100.0 μM) at GC|SWCNT|**1** electrode.

interferences. As expected, in the presence of glutathione, the quantification of cysteine is limited, disturbed or stopped, which is to be expected since glutathione is a thiol-containing compound and therefore can also be oxidized with Cu^{2+}. Figure 5 shows the effect of different concentrations of vitamin C (50–100 μM) on the anodic current in the presence of 50.0 μM Cys-SH. The presence of vitamin C results in an additional anodic peak at 550 mV (the oxidation peak of vitamin C) which partly overlaps with that of Cys-SH, causing significant interferences (+5 %) at a vitamin C concentration of 0.1 mM. It was also found that 200-fold amount of *L*-alanine and isoleucine (as non-thiol amino acids) did not affect the signal response. In a solution containing 10.0 μM cysteine, the addition of lauric acid and EDTA up to 100 μM also did not affect the response of the electrode to cysteine.

The repeatability of the proposed method using the GC|SWCNT|**1** electrode within one day was investigated by ten consecutive measurements of Cys-SH in a solution containing 10 μM analyte using the same electrode. Determined relative standard deviation (RSD) of 10.7 % indicates good repeatability and a stable response, which opens up the possibility of using GC|SWCNT|**1** for electroanalytical purposes. Reproducibility (4.8 %) was determined using five freshly prepared GC|SWCNT|**1** electrodes over 5 days.

CONCLUSIONS

Electrochemical characterization of a hydrothermally synthesized copper(II) coordination compound characterized by elemental analysis, ESI-MS, MALDI-TOFMS, FT-IR spectroscopy and thermogravimetric analysis was carried out to find a sensitive and simple method to improve the determination of biologically active thiol substances using cysteine as an example under biological conditions.

For the three main mass-to-charge ratio peaks obtained from ESI mass spectra of the coordination compound **1**; at *m*/*z* 282 amu assigned to 2 $Na^+[Cu(L)(H_2O)_2]$, at *m* / *z* 381 amu assigned to 2 $Na^+[Cu(L)_2]^{2-}$ and at *m* / *z* 723 amu assigned to $\{[Cu(L)_2(OH_2)]\}_2$, structures have been proposed. MALDI-TOF mass spectra reveal one main most abundant peak attributed to$[Cu(L)(H_2O)_2]_2$.

Based on DTA/TGA curves and IR spectra, chelating *O*, *O*-coordination (through the oxygen atom of the carboxyl group and the oxygen atom of the amide group) of keto(amide) tautomer of 2-OHnicH were supposed in the complex compound **1**.

The electrochemical studies of synthesized complex suggest improving electron exchange due to the presence of |SWCNT|**1** on the electrode since copper oxidation (as redox-active metal center) as well as the reduction of the 2-OHnicH ligand, according to the proposed semi-reduction reaction, appears as clear peaks.

The proposed concept of the method of electrochemical analysis of cysteine based on the anodic peak of $Cu(S\text{-}Cys)_2$ complex, suggests the possibility of cysteine detection and proposes the development and improvement of this innovative sensor. From the results mentioned above, we can conclude that the GC|SWCNT|**1** electrode exhibits highly electrocatalytic activity toward Cys-SH oxidation. Under the electrochemical conditions used, a linear response, *i.e.*, a linear increase in the peak anodic currents of $Cu(S\text{-}Cys)_2$ with the concentration of Cys-SH in the range of 0.2–20 μM, and a low detection limit of 0.09 μM were obtained. The modified electrode offers higher selectivity in voltammetric measurements of Cys-SH. The new sensor provides a promising platform for the construction of sensors based on coordination compounds for future applications in electrocatalysis.

Further systematic work is underway to obtain crystals suitable for single crystal X-ray diffraction analyses.

Acknowledgment. The authors gratefully acknowledge Sonja Miladić, student and Mag. Dr. Miljan Milunović, MSc from the University of Vienna, Fakultät für Chemie, Institut für Anorganische Chemie, Austria for their contribution to obtain elemental analysis and MALDI -TOF-MS measurement.

Supplementary Information. Supporting information to the paper is attached to the electronic version of the article at: https://doi.org/10.5562/cca3939.

PDF files with attached documents are best viewed with Adobe Acrobat Reader which is free and can be downloaded from Adobe's web site.

REFERENCES

[1] Z. Ming-Hua, W. Mei-Chun, Z. Li-Hong, L. Hong, Y. Xu-Wu, *Chin. J. Chem.* **2007**, *25*, 6–19. https://doi.org/10.1002/cjoc.200790010

[2] X. M. Chen, M. L. Ton, *Frontiers in Crystal Engineering*, John Wiley & Sons, USA: Ltd; **2006**, pp. 223–266.

[3] J-Z. Gao, J. Yang, Y-Y. Liu, J-F. Ma, *Cryst. Eng. Comm.* **2012**, *14*, 8173–8185. https://doi.org/10.1039/C2CE25953B

[4] W. H. Zhang, Y. Y. Wang, E. K. Lermontova, G. P. Yang, B. Liu, J. C. Jin, Z. Dong, Q. Z. Shi, *Cryst. Growth Des.* **2010**, *10*, 76–84. https://doi.org/10.1021/cg900285b

[5] Y. Q. Wang, W. W. Sun, Z. D. Wang, Q. X. Jia, E. Q. Gao, Y. Song, *Chem. Commun.* **2011**, *47,* 6386–6388. https://doi.org/10.1039/C1CC12028J

[6] L. Lu, W. Jun, W. Wei-Ping, Z. Xiu-Lan, X. Bin, *Synth. React. Inorg. Met-Org. Nano-Met. Chem.* **2014**, *44*, 393–396. https://doi.org/10.1080/15533174.2013.771669

[7] J. Q. Liu, Y. S. Huang, D. H. Xu, *Synth. React. Inorg. Met-Org. Nano-Met. Chem.* **2012**, *42*, 1115–1119. https://doi.org/10.1080/15533174.2012.680153

[8] Y. R. Liu, Y. T. Pan, *Synth. React. Inorg. Met-Org. Nano-Met. Chem.* **2009**, *39*, 685–689. https://doi.org/10.1080/15533170903433204

[9] Y.-Y. Liu, J. Yang, J.-F. Ma, *Z. Anorg. Allg. Chem.* **2014**, *640*, 2217–2225. https://doi.org/10.1002/zaac.201400206

[10] D. Niu, J. Yang, J. Guo, W.-Q. Kan, S.-Y. Song, P. Du, J.-F. Ma, *Cryst. Growth Des.* **2012**, *12*, 2397−2410. https://doi.org/10.1021/cg3000526

[11] J. R. Long, O. M. Yaghi, *Chem Soc Rev.* **2009**, *38*, 1213–1214. https://doi.org/10.1039/B903811F

[12] H. H. Zou, S. H. Zhang, Y. Xiao, C. Feng, Y. Guang Wang, *Struct. Chem.* **2011**, *22*, 135–140. https://doi.org/10.1007/s11224-010-9684-9

[13] C. L. Ma, Q. Li, R. F. Zhang, *Inorg. Chim. Acta* **2009**, *362*, 2937–2940. https://doi.org/10.1016/j.ica.2008.11.016

[14] Y Lü, X Zhang, X-B Cui, J.-Q. Xu, *Inorg. Chem.* **2018**, *57*, 11123–11134. https://doi.org/10.1021/acs.inorgchem.8b01705

[15] J. Zubieta, *Applications of hydrothermal synthesis to solid state coordination chemistry*. In *Comprehensive coordination chemistry* II, McCleverty JA, Meyer TJ, editors. Elsevier Science, **2003**, p. 697.

[16] C. Santini, M. Pellei, V. Gandin, M. Porchia, F. Tisato, C. Marzano, *Chem. Rev.* **2014**, *114*, 815−862. https://doi.org/10.1021/cr400135x

[17] S. A. Khan, S. Kanwal, A. Iqbal, W. Ahmad, *Int. J. Adv. Res.* **2017**, *5*, 1350–1368. https://doi.org/10.21474/IJAR01/3959

[18] J. Miklovič, P. Segľa, D. Mikloš, J. Titiš, R. Herchel, M. Melník, *Chem Pap.* **2008**, *62*, 464–471. https://doi.org/10.2478/s11696-008-0056-5

[19] V. Jorík, E. Scholtzová, P. Segl'a, *Z. Kristallogr.* **2008**, *223*, 524–529. https://doi.org/10.1524/zkri.2008.0057

[20] J. Jašková, D. Mikloš, M. Korabik, V. Jorík, P. Segl'a, B. Kaliňáková, D. Hudecová, J. Švorec, A. Fischer, J. Mrozinski, T. Lis, M. Melník, *Inorg. Chim. Acta* **2007**, *360*, 2711–2720. https://doi.org/10.1016/j.ica.2007.01.022

[21] F. A. Al-Saif, M. S. Refat, *J. Mol. Str.* **2012**, *1021*, 40–52. https://doi.org/10.1016/j.molstruc.2012.04.057

[22] P. Segl'a, D. Mikloš, J. Jaškova, J. Miklović, B. Kalinakova, D. Hudecova, J. Švorec, T. Lis, M. Melnik, *J. Coord. Chem.* **2008**, *61*, 3763–3775. https://doi.org/10.1080/00958970802146049

[23] T. A. Ban, *Prog. Neuro-Psychoph.* **2001**, *25*, 709–727. https://doi.org/10.1016/S0278-5846(01)00160-9

[24] R. H. Salama, A. Y. Nassar, A. A. Nafady, H. H. Mohamed, *Liver Int.* **2007**, 454–464. https://doi.org/10.1111/j.1478-3231.2007.01460.x

[25] T. Suksrichavalit, S. Prachayasittikul, T. Piacham, C. Isarankura-Na-Ayudhya, C. Nantasenamat, V Prachayasittikul, *Molecules* **2008**, *13*, 3040–3056. https://doi.org/10.3390/molecules13123040

[26] M. A. Al-Anber, *Am. J. Phys. Chem.* **2013**, *2*, 1–7. https://doi.org/10.11648/j.ajpc.20130201.11

[27] B. Filanovsky, *Anal. Chim. Acta.* **1999**, *394*, 91–100. https://doi.org/10.1016/S0003-2670(99)00035-5

[28] A. A. Ensafi, S. Behyan, *Sens. Actuat. B* **2007**, *122*, 282–288. https://doi.org/10.1016/j.snb.2006.05.035

[29] A. Salimi, R. Hallaj, *Talanta* **2005**, *66*, 967–975. https://doi.org/10.1016/j.talanta.2004.12.040

[30] L. P. Liu, Z. J. Yin, Z. S. Yang, *Bioelectrochemistry* **2010**, *79*, 84–89. https://doi.org/10.1016/j.bioelechem.2009.12.003

[31] N. S. Lawrence, J. Davis, R. G. Compton, *Talanta* **2001**, *3,* 1089–1094. https://doi.org/10.1016/S0039-9140(00)00579-8

[32] N. Vladislavić, S. Brinić, Z. Grubač, M. Buzuk, *Int. J. Electrochem. Sci.* **2014**, *9,* 6020–6032.

[33] A. M. Mahmoud, S. A. Alkahtani, M. M. El-Wekil, *Anal Bioanal Chem.* **2022**, *414*, 2343–2353. https://doi.org/10.1007/s00216-021-03852-0

[34] N. Vladislavić, I. Škugor Rončević, M. Buzuk, M. Buljac, I. Drventić, *J. Solid State Electrochem.* **2021**, *25*, 841−857. https://doi.org/10.1007/s10008-020-04856-z

[35] G. Alarcón-Angeles, B. Pérez-López, M. Palomar-Pardave, M. T. Ramírez-Silva, S. Alegret, A. Merkoçi, *Carbon* **2008**, *46,* 898–906. https://doi.org/10.1016/J.CARBON.2008.02.025

[36] A. Merkoçi, *Microchim. Acta* **2006**, *152*, 155–156. https://doi.org/10.1007/s00604-005-0450-4

[37] D. Krivić, N. Vladislavić, M. Buljac, I. Škugor Rončević, M. Buzuk, *J. Electroanal. Chem.* **2022**, *907*, 116008. https://doi.org/10.1016/j.jelechem.2021.116008

[38] I. Škugor Rončević, N. Vladislavić, N. Chatterjee, V. Sokol, C. L. Oliver, B-M. Kukovec, *Chemosensors* **2021**, *9*, 352. https://doi.org/10.3390/chemosensors9120352

[39] B. Kozlevčar, P. Šegedin, *Croat. Chem. Acta* **2008**, *81*, 369–379.

[40] D. İnci, R. Aydın, Ö. Vatan, T. Sevgi, D. Yılmaz, Y. Zorlu, Y. Yerli, B. Çoşut, E. Demirkan, N. Çinkılıç, *J. Biol. Inorg. Chem.* **2017**, *22*, 61–85. https://doi.org/10.1007/s00775-016-1408-1

[41] M. F. Wyatt, *J. Mass. Spectrom.* **2011**, *46*, 712–719. https://doi.org/10.1002/jms.1957

[42] K. Nakamoto Infrared, *Raman spectra of inorganic, coordination compounds,* 6th ed. part B, Wiley, New York, **2009**, pp. 62–67.

[43] L. Kucková, K. Jomová, A. Švorcová, M. Valko, P. Segľa, J. Moncoľ, J. Kožíšek, *Molecules* **2015**, *20*, 2115–2137. https://doi.org/10.3390/molecules20022115

[44] W. Jun, W. Wei-Ping, L. Lu, X. Bin, *J. Mol. Struct.* **2013**, *1036*, 174–179. https://doi.org/10.1016/j.molstruc.2012.09.075

[45] B. Nigović, S. Behetić, *Farm. Glas.* **2007**, *63*, 163–175.